International Journal for Parasitology: Parasites and Wildlife 25 (2024) 101002

Contents lists available at ScienceDirect

International Journal for Parasitology: Parasites and Wildlife

journal homepage: www.elsevier.com/locate/ijppaw

Exploring the anatomy of *Linguatula serrata* using micro-computed tomography

Alice Birckhead [a,*], Ryan O'Hare Doig [b], Ann Carstens [a,c], David Jenkins [a], Shokoofeh Shamsi [a,d,**]

[a] School of Agricultural, Environmental and Veterinary Sciences, Charles Sturt University, Wagga Wagga, Australia
[b] Preclinical, Imaging and Research Laboratories, South Australian Health and Medical Research Institute (SAHMRI), Adelaide, South Australia, Australia
[c] Department of Companion Animal Clinical Studies, Faculty of Veterinary Sciences, University of Pretoria, Onderstepoort, South Africa
[d] Gulbali Institute, Charles Sturt University, Australia

ARTICLE INFO

Keywords:
Pentastomida
Tongue worm
Parasite
Dog
Micro-CT

ABSTRACT

Micro-computed tomography (micro-CT) is an emerging tool in parasitology that can assist in analysing morphology and host-parasitic interactions. It is a non-destructive, cross-sectional imaging technique that offers good resolution and the ability to create three-dimensional (3D) reconstructions. Here, we used micro-CT to study *Linguatula serrata*, which is a zoonotic pentastome parasite that infects dogs and ruminants throughout the world. The aims of this study were to describe the internal and external anatomy of adult *L. serrata* specimens using micro-CT, and to describe and compare specimens stained with 0.3% phosphotungstic acid (PTA) and 1% iodine (I_2). Ten adult *L. serrata* specimens were subjected to micro-CT examination. The specimens were fixed in 70% ethanol and stained with 0.3% PTA or 1% I_2. Both stains offered good tissue contrast. The main identifying external features of *L. serrata* (hooks, mouth, buccal cadre) were clearly visible. Virtual sections and 3D reconstructions provided a good overview of the coelomic cavity, with visualisation of the digestive tract, nervous system, and male and female reproductive organs. These micro-CT images and morphological descriptions may serve as an anatomical reference for *L. serrata*, in particular, the internal anatomy which has not been described in recent years.

1. Introduction

Micro-computed tomography (micro-CT) is a promising and underutilised technique in parasitology and can be used to elucidate taxonomy (Tessler et al., 2016; O'Sullivan et al., 2018). It is a non-destructive technique that offers high image resolution, and when used in conjunction with tissue stains, good image contrast of soft tissues can be achieved (Metscher, 2009; Gignac et al., 2016). External and internal anatomy can be visualised, in different planes and in three dimensions (3D) (Tessler et al., 2016; Parapar et al., 2017). Micro-CT in combination with various stains has been used to classify a range of soft bodied organisms, including earthworms, leeches, and other annelids (Fernández et al., 2014; Tessler et al., 2016; Parapar et al., 2017); as well as to study numerous insects (Smith et al., 2016; Rother et al., 2021; Giglio et al., 2022). Micro-CT can also provide useful information on host-parasitic interactions through visualisation of parasites *in situ* (Lee et al., 2007; Noever et al., 2016; O'Sullivan et al., 2021).

Linguatula serrata (tongue worm) is a zoonotic pentastome arthropod parasite that infects domestic and wild carnivores and herbivores (Christoffersen and De Assis, 2013; Attia et al., 2024). Although the parasite has a global distribution, tongue worms are generally underdiagnosed and their true prevalence is unknown (Tabaripour et al., 2019, 2021). Recently, tongue worms were found to be highly prevalent in wild canids in south-eastern Australia (Shamsi et al., 2017) as well as in a range of native and introduced hosts (Barton et al., 2019, 2020, 2021; Shamsi et al., 2020; Barton et al., 2022, b).

Adult tongue worms live in the upper respiratory tract of canids and vulpids. They have a distinctive appearance, with a flattened 'tongue-like' annulated body and two pairs of retractile hooks at the anterior end (Paré, 2008). While tongue worms are readily identifiable to the genus

* Corresponding author. School of Agricultural, Environmental and Veterinary Sciences, Charles Sturt University, Locked Bag 588, Wagga Wagga, NSW, 2678, Australia.
** Corresponding author. School of Agricultural, Environmental and Veterinary Sciences, Charles Sturt University, Wagga Wagga, Australia.
E-mail addresses: abirckhead@csu.edu.au (A. Birckhead), sshamsi@csu.edu.au (S. Shamsi).

https://doi.org/10.1016/j.ijppaw.2024.101002
Received 19 August 2024; Received in revised form 8 October 2024; Accepted 11 October 2024
Available online 12 October 2024

level, the lack of morphological information about *Linguatula* species and their developmental stages, has meant that *L. serrata* has sometimes been misidentified (Barton et al., 2022; Shamsi et al., 2022). Scanning electron microscopy (SEM) has provided more detailed information about the external features of *L. serrata* (Shamsi et al., 2020), and molecular markers for *Linguatula* species have also been identified (Shamsi et al., 2022). Ideally, a combined morphological and molecular approach is needed when diagnosing *Linguatula* species (Shamsi et al., 2022; Attia et al., 2024).

There are only a few publications describing the internal anatomy of *L. serrata* or pentastomes generally; most are decades old and some are not written in English (Spencer, 1892; Sambon, 1922; Haffner et al., 1969; Mehlhorn, 2008; von Vaupel Klein, 2015). Rezaei et al. (2016) provide some mensuration values of the intestine and uterus in *L. serrata* specimens, but not a detailed morphological description of the internal anatomy. Characterising tongue worms based on measurements is not recommended, as features such as the size of the hooks, buccal cadre, and copulatory spicule are found to be highly variable in different geographic locations and may be influenced by host factors (Barton et al., 2022). *L. arctica* was examined by SEM combined with dissection, and components of the female reproductive system and intestine were described (Nikander and Saari, 2006). The external anatomy of *L. serrata* specimens from Australia, Romania, and Iran has also been described (Rezaei et al., 2016; Shamsi et al., 2020; Barton et al., 2022).

We recently used conventional CT to describe *L. serrata* (Birckhead et al., 2024). CT captured the generally broad and elongated body shape of the tongue worms, and an outer hyperattenuating rim in the females, which was speculated to be due to their chitinous exoskeleton. The spatial resolution was not high enough to visualise smaller external details, such as hooks or their internal anatomy. The aims of this paper are to document the internal and external anatomy of *L. serrata* using micro-CT, and to explore how image detail and stain uptake vary with the use of 0.3% phosphotungstic acid (PTA) and 1% iodine (I_2) stains. While the technique and stains utilised in the study are well documented in the literature, to our knowledge, this is the first time micro-CT has been used to examine a pentastome parasite and *L. serrata* specifically.

2. Material and methods

2.1. Linguatula serrata collection and sample preparation

Linguatula serrata specimens were retrieved at necropsy examination of wild canid (dingoes [*Canis lupus dingo*] and dingo/dog hybrids) and vulpid (*Vulpes vulpes*) cadavers supplied by professional vertebrate control officers, as previously described (Shamsi et al., 2017; Birckhead et al., 2024). The canids and vulpids were trapped and shot in the Kosciusko National Park area and the Southern Tablelands region, New South Wales, Australia, between September 2017 and May 2023, as part of vertebrate pest management. Cadaver heads were bagged, labelled and frozen within 12 h of death, and stored until post-mortem examination. Retrieved tongue worms were placed immediately in 70% ethanol and stored until they were examined by micro-CT. Ten tongue worm specimens were selected for micro-CT. They consisted of seven females (ranging from 27 to 87 mm in length, and a juvenile female of 15 mm length) and three males (16–22 mm in length). The intention was to scan four males; however, one specimen was determined to be a juvenile female on micro-CT. Three female and two male specimens were stained with 0.3% phosphotungstic acid (PTA) and four females and one male specimen with 1% iodine metal (I_2). Stain formulations and protocols followed those previously described (Metscher, 2009) (Table 1). Specimens were sealed in Eppendorf plastic tubes, and physically anchored using low-density polystyrene foam specimen holders to prevent movement during scanning (Fig. 1).

Table 1
Phosphotungstic acid (PTA) and iodine (I_2) staining protocols used on the tongue worm specimens adapted from (Metscher, 2009).

Stain	Stock Solution	Staining procedure
PTA	1% (w/v) PTA in water (dedeca Tungstophosphoric acid hydrated; Chem supply Australia)	Samples held in fresh 70% ethanol (EtOH) overnight. Samples added to 0.3% PTA solution with 70% EtOH. Samples left in staining solution for 72 h, at room temperature, gently agitated via rocking plate. Samples taken to 70% EtOH for 30 min, then 100% EtOH. Samples scanned in 100% EtOH.
I2E	1% iodine metal (inorganic iodine, Chem Supply Australia) dissolved in 100% ethanol (I_2E)	Samples taken to 100% alcohol overnight. Samples added to I_2E solution for 72 h, at room temperature, gently agitated via rocking plate. Samples washed with 100% alcohol 2–3 times until free iodine was not visible. Samples scanned in 100% EtOH.

2.2. Micro-computed tomography and analysis

High-resolution three-dimensional micro-CT scanning and analysis were performed at the Small Animal Imaging Facility of the South Australian Health and Medical Research Institute (SAHMRI, Adelaide, South Australia). A total of ten *L. serrata* specimens underwent micro-CT (SkyScan 1176; Bruker) at a nominal resolution of 9, 18, or 35 μm, 30–470 ms exposure, 1, 2, or 4K pixelation (camera binning mode). An X-ray tube voltage of 55 kV and 413 μA was applied, with no filter. The scan orbit was 360° with a rotation step of 0.3, 0.5, or 0.8° and 2-frame averaging (see Appendix 1 for full scanning parameters). Reconstruction of the micro-CT scans was carried out with a modified Feldkamp algorithm using SkyScan NRecon software (Version 1.7.4.2), accelerated with the GPU Recon Server Reconstruction engine (Version 1.7.4), applying Guassian smoothing (2), ring artifact reduction (10), and beam hardening correction (30%) to all samples.

The micro-CT files were processed with ORS Dragonfly (software version 2022,2.0.1399). Two-dimensional (2D) imaging slices were evaluated in different planes and still images were captured in transversal, sagittal, and frontal planes, using the specimens that were of highest quality and most representative. 3D reconstructions and volumetric rendering were also performed.

The anatomical terminology used in the results and discussion sections follows that of Mehlhorn (2008) and von Vaupel Klein (2015). Image quality of tongue worm specimens stained with 0.3% PTA and 1% I_2 was assessed and compared for detail, stain uptake, contrast between organs, visualisation of anatomical structures, and for the presence of artifacts such as movement blur.

3. Results

3.1. Image quality

Two *L. serrata* specimens were initially micro-CT scanned unstained in ethanol but image contrast was poor, and these scans were not analysed. Image detail was notably poorer at a scanning resolution of 35 μm compared to at 18 μm and 9 μm, for both contrast staining techniques (Fig. 2). Therefore, 18 μm and 9 μm were used for the anatomical analyses and representative 3D volumes. External and internal anatomical features could be visualised with both the 0.3% PTA and 1% I_2 stains. Internal organ contrast was generally comparable with both stains, other than the ovary being slightly more contrast-enhancing with the 0.3% PTA stain. Some differences in external detail were noted between the stains. The hooks and buccal cadre, and copulatory spicules were more

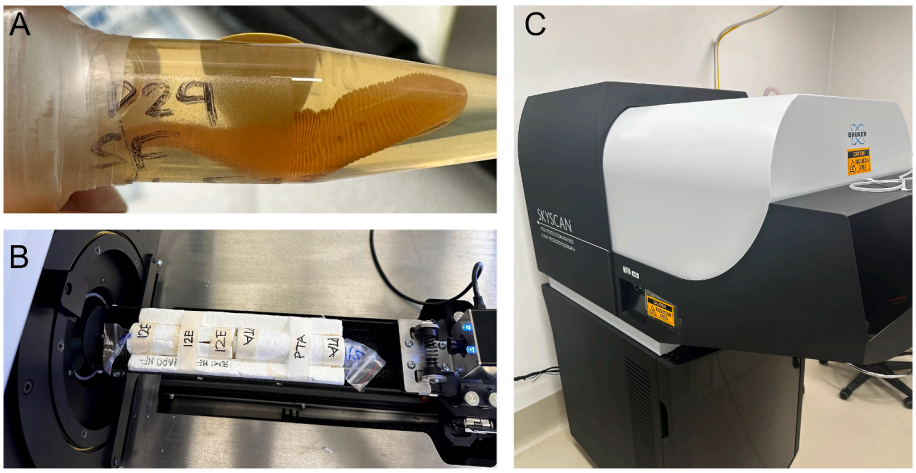

Fig. 1. (A) Photograph of a small female tongue worm specimen stained with 0.3% PTA in an Eppendorf tube, prepared for micro-CT scanning. (B) The Eppendorf tubes were held in place in a foam specimen holder during micro-CT scanning. (C) A photograph of the micro-CT machine used.

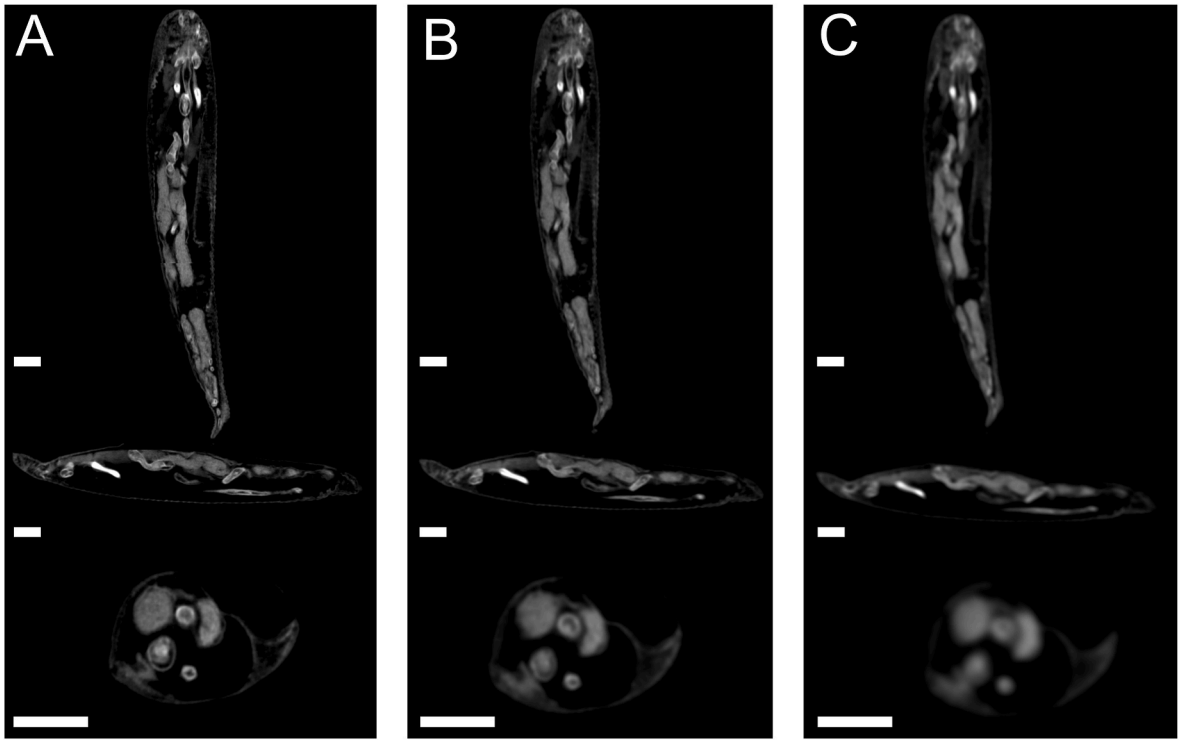

Fig. 2. Ventral (top), sagittal (middle) and transversal views (bottom) of a male tongue worm stained with 0.3% PTA at scanning resolutions of 9 μm (A), 18 μm (B), and 35 μm (C). The image detail is notably poorer at 35 μm compared to other scanning resolutions, especially when magnified. The anterior end is at the top of the image (ventral views) or to the left (sagittal views). White bar = 1 mm.

contrast-enhancing and clearly defined with the 1% I_2 stain compared to the 0.3% PTA stain (Fig. 3). External cuticle detail in the female was generally better with the 0.3% PTA stain, with a greater range of contrast observed.

Internal features that were strongly hyperattenuating or contrast-enhancing with both stains, were the uterus filled with eggs and the ejaculatory ducts (in the male). The digestive tract, the ovaries, and testes were moderately contrast-enhancing. The coelomic space or haemocoel was hypoattenuating.

Artifacts consisted of poor stain uptake in one male and one female specimen stained with 0.3% PTA (Fig. 4A). Image quality in the male specimen was particularly poor, resulting in the image dataset not being analysed. Movement blur was seen in one female specimen (Fig. 4B); this parasite was subsequently rescanned, and the problem was rectified. In another female specimen (Fig. 5A-B), the head had an undulating contour. The cause was unknown, but possibly associated with the positioning in the container, a fixation artifact, or damage sustained during retrieval of the parasite at necropsy.

Fixation time in 70% ethanol prior to the micro-CT scan, ranged from 12 to 14 days (two male and four female specimens) to 4–5 years (one male and three female specimens). No obvious differences in image quality and stain uptake were observed between these specimens (Fig. 6).

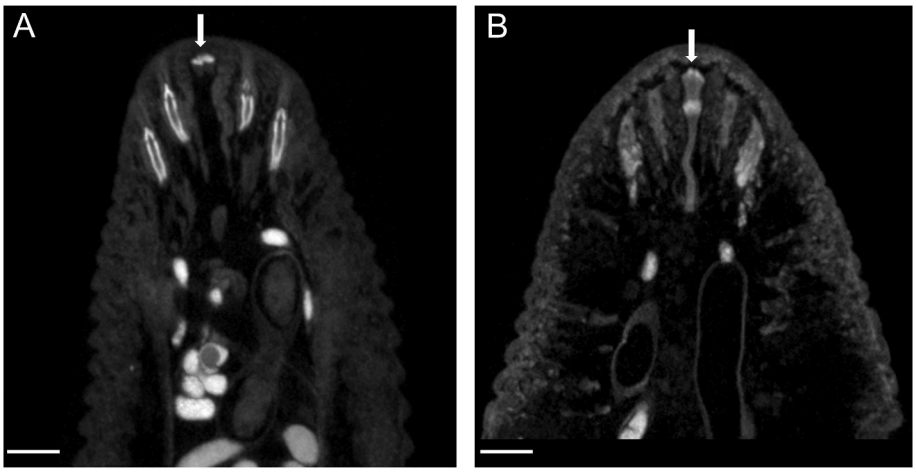

Fig. 3. Ventral views of the anterior end of two female tongue worms scanned at 18 μm resolution, and stained with 1% I_2 (A) or 0.3% PTA (B). The buccal cadre (arrow) and hooks (either side) are more contrast-enhancing and clearly defined with the 1% I_2 stain. A greater range of contrast is seen with the 0.3% PTA stain. The anterior end is at the top of the image. White bar = 1 mm.

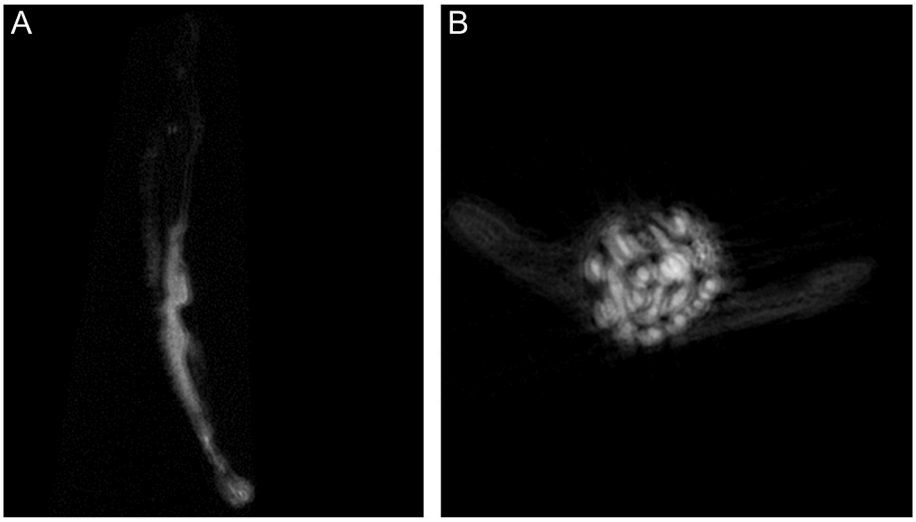

Fig. 4. (A) Dorsal view of a male tongue worm specimen stained with 0.3% PTA, demonstrating poor stain uptake artifact (anterior end is to the top of the image). (B) Transversal view of a female specimen stained with 1% I_2, demonstrating movement blur artifact.

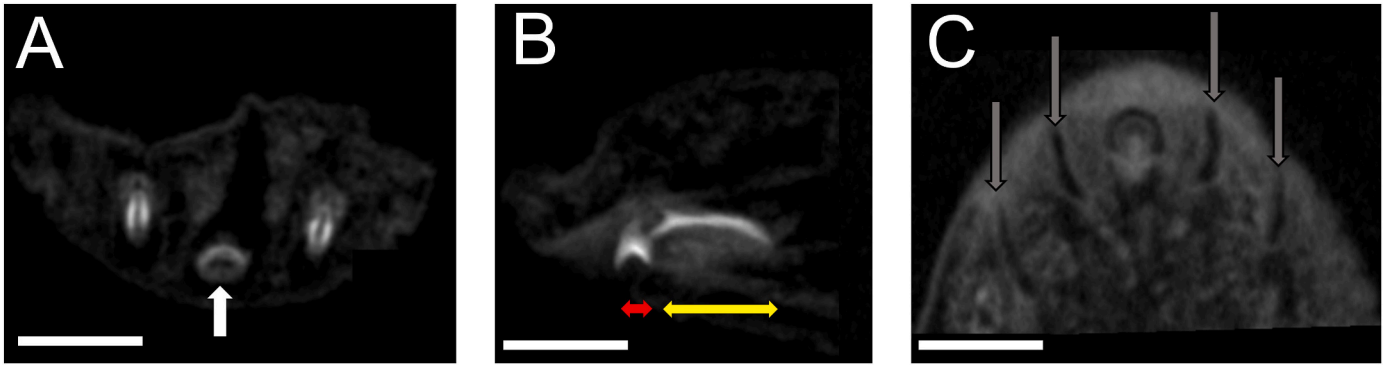

Fig. 5. Transversal (A) and sagittal (B) views of the anterior end of a female tongue worm specimen stained with 1% I_2 and scanned at 18 μm resolution. In A, the tips of the anterior hooks are visible on either side of the mouth (white arrow). In B, an anterior hook is visible. The red arrow corresponds to the hook and the yellow to the fulcrum. Note the undulating contour of the dorsal aspect of the head (cause unknown; likely artifactual). (C) Ventral view of a female specimen stained with 0.3% PTA and scanned at 9 μm resolution, showing the hook pits (grey arrows). Anterior is to the left (sagittal image) or the top (ventral image). White bar = 1 mm. (For interpretation of the references to colour in this figure legend, the reader is referred to the Web version of this article.)

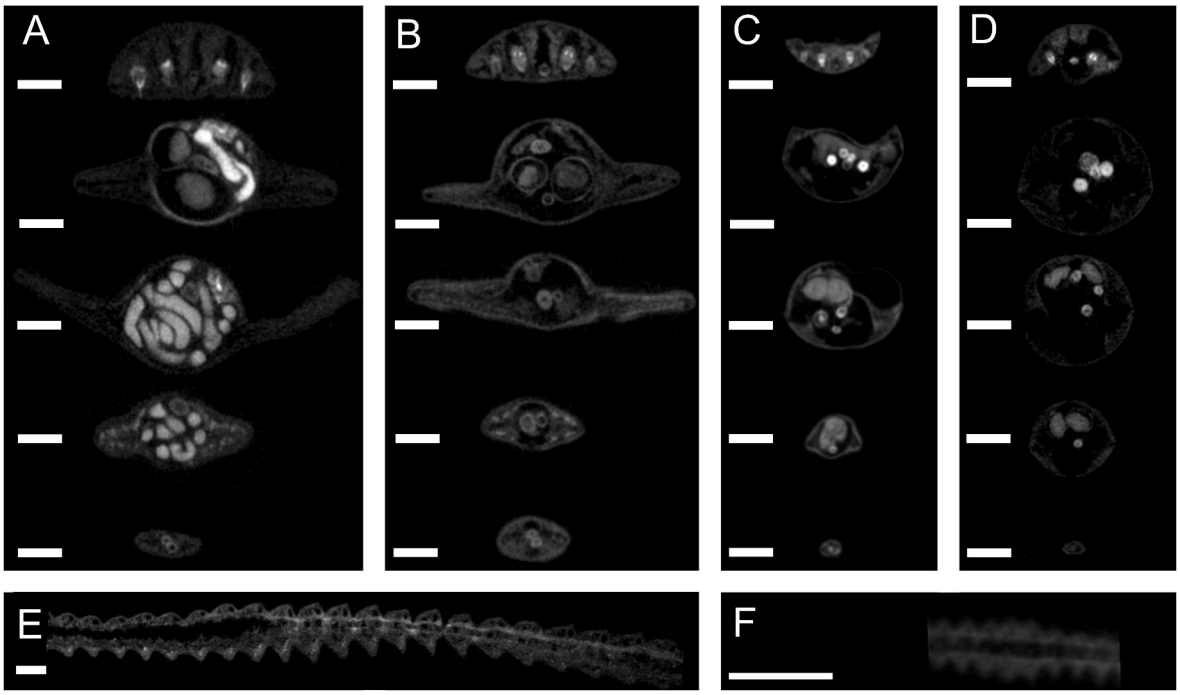

Fig. 6. Transversal views of female (A and B) and male (C and D) tongue worm specimens, from anterior to posterior end (top to bottom). Note the pronounced lateral lobes in the females and the generally rounder body shape in the male. Specimens in A, B and D were stained with 1% I_2, and C was stained with 0.3% PTA. No noticeable difference in stain uptake was observed in specimens fixed in ethanol for 4–5 years (specimens A and C) compared to those fixed in ethanol for 12–14 days prior to the micro-CT scan (specimens B and D). E and F, sagittal views of the lateral lobe of a female (E) and male (F) tongue worm stained with 0.3% PTA, showing their serrated contours. Scanning resolution of all images is 18 μm, except for F, which is 9 μm. The anterior is to the left for the sagittal views. White bar = 1 mm.

3.2. Morphological features

3.2.1. External features

The two pairs of sharply pointed hooks, mouth, and buccal cadre at the anterior end of the parasite were readily identified (Fig. 3, 5A-B, & 7E). The hooks had a hyperattenuating rim and hypoattenuating centre. Hook pits were observed as hypoattenuating slits (Fig. 5C).

The female tongue worms had a broad dorsoventrally flattened anterior body and a narrow rounded posterior end (Fig. 6A-B & 7A-B). The head generally had a smoothly convex dorsal margin. Fine external

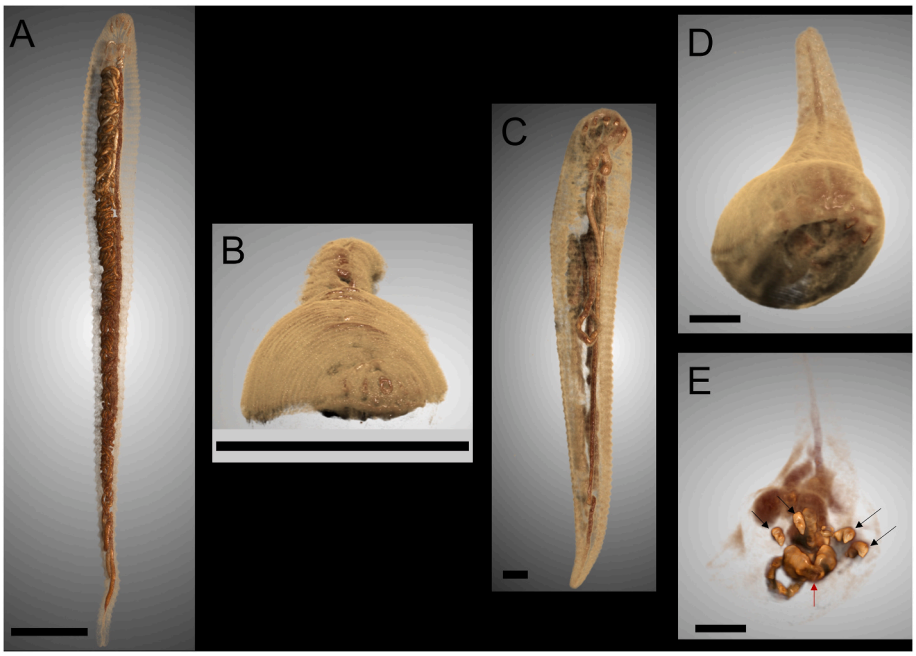

Fig. 7. 3D reconstructions of female (A & B) and male (C, D & E) tongue worm specimens stained with 1% I_2 and scanned at a resolution of 18 μm. A & C are ventral views, and B, D, and E are frontal views of the head; volumetric rendering in the latter highlights the hooks (black arrows) and copulatory spicules (red arrow) of the male. The anterior end is at the top of the image for the ventral views. Black bar in A & B = 10 mm; and in C, D, & E = 1 mm. (For interpretation of the references to colour in this figure legend, the reader is referred to the Web version of this article.)

annuli were identified throughout the body. The lateral margins or lobes of the anterior body had a serrated contour (Fig. 6E). The two male tongue worms had similarly dorsoventrally flattened heads as the females; one had a smoothly convex dorsal margin and the other had pointed lateral margins. The male body shape was generally rounder than the female, and prominent lateral lobes were not observed (Fig. 6C-D & 7C-D). Fine external serrations, similar to the female, were present (Fig. 6F).

3.2.2. *Digestive system*

Bands of moderately contrast-enhancing tissue were present in the dorsal head region, on either side of the hooks and mouth, which is likely consistent with musculature and glandular tissue (Fig. 8A-B).

The buccal cavity, oesophagus, and intestine were clearly visible (Fig. 8C-D). The buccal cadre extended a similar depth to its width. The oesophagus, a thin hollow tube, arose immediately posterior to the buccal cadre. It ran in a horizontal direction before turning dorsally to join the intestine (or midgut). The pharynx was not clearly defined but was mildly thicker and more contrast-enhancing than the oesophagus. The junction between the oesophagus and intestine was clearly defined, with a concentric ring (valve). The intestine was approximately five times the diameter of the oesophagus. In females the intestine was generally filled with moderately contrast-enhancing and slightly heterogeneous material (ingesta). The intestine in the male was relatively thinner for its body size. The intestine continued as a relatively straight tube in a posterior direction, gradually narrowing and terminating at the most posterior part of the body, at the anus. In females, the anus was just dorsal to the genital pore. A hindgut or posterior intestine was not differentiated from the midgut.

3.2.3. *Female reproductive system*

The ovary was a long structure that extended approximately two-thirds of the body, dorsally and lateralised to one side of the coelomic cavity (Fig. 9A-B & H). The ovary was moderately heterogeneously contrast-enhancing and had a cobbled appearance. The very anterior aspect of the ovary bifurcated into two narrow oviduct tubes that contained several small, round, luminal hyperattenuating/contrast-enhancing structures (likely consistent with ova; Fig. 9A). The tubes extended anterolaterally along the body walls and fused ventrally, at the level of the junction of the oesophagus and intestine (Fig. 9C). The fused tube continued midline, ventral to the intestine and between the two receptacula seminis, and then posteriorly as the uterus. The ovary could not be identified in one young female *L. serrata* specimen.

The receptacula seminis were observed as two elongated, blind-ended tubular structures that were located midline and ran in a posterior direction (Fig. 9C-D, F-G). Intraluminally, they contained a variable amount of clumped hyperattenuating material (consistent with spermatozoa). A thin tube or ductule arose from the anterior aspect of each of the receptaculum seminis, coursed medially and joined the fused oviduct tube.

The uterus was highly coiled and looped around the relatively straight intestine, and filled much of the coelomic cavity (Fig. 9B, E, & H). The uterine lumen was variably filled with intensely hyperattenuating or contrast-enhancing material, and individual eggs were not clearly visible. In two mature females, the uteri were relatively empty. The uterus in the young female examined was narrower, less coiled and did not contain any hyperattenuating material (Fig. 9G).

Image detail was generally reduced in the posterior end of the parasites due to the narrow size and reduced stain uptake. The vagina was a continuation of the most posterior aspect of the uterus and appeared as a short, narrow empty tube. The genital pore was immediately ventral to the anus and was observed as a small opening.

3.2.4. *Male reproductive system*

The two testes appeared as elongated, homogeneously attenuating, undulating structures that were surrounded by a thin membrane and extended dorsally along almost the entire length of the body (Fig. 10A & E). A single seminal vesicle tube originated from the anterior aspects of the testes and contained moderately contrast-enhancing luminal material. It was slightly variable in diameter, with two dilatations observed in the distal segment (Fig. 10D). The seminal vesicle had a slightly tortuous course. It extended in a posterior direction between the testes, turned tightly in the ventral aspect of the mid coelomic cavity, and ran anteriorly down the midline to the level of the proximal intestine (Fig. 10E). The seminal vesicle bifurcated at the proximal intestine into two short, narrow-diameter tubes. These tubes ran ventrally and connected with the two short vas deferens, anteriorly, and the two ejaculatory ducts, posteriorly. The vas deferens continued anteriorly to the cirrus sac. The ejaculatory ducts were observed as thick-walled, strongly contrast-enhancing, blind-ended, tubular structures, that were slightly undulating and horizontally orientated (Fig. 10C & E). The two copulatory spicules were clearly defined, with strongly contrast-enhancing rims. The posterior aspect was rounded, and the anterior aspect was more pointed (Fig. 10B-C & E). The paired penes (cirri) within the cirrus sac were not clearly visible. The genital pore opening was seen at the ventral aspect of the anterior cephalothorax (Fig. 10D).

3.2.5. *Nervous system*

The suboesophageal ganglion was visualised with micro-CT (Fig. 11). The most anterior part of the suboesophageal ganglion

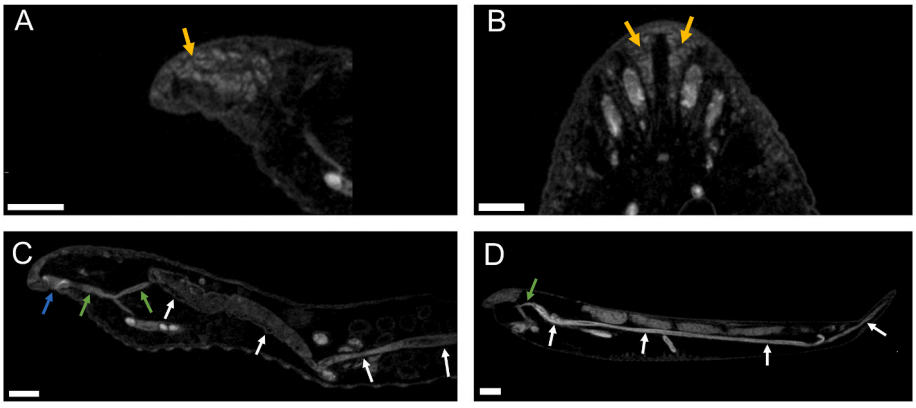

Fig. 8. Sagittal (A) and ventral views (B) of the anterior aspect of a female tongue worm specimen stained with 0.3% PTA, highlighting moderately contrast-enhancing bands of tissue of the head (yellow arrows). These are likely consistent with musculature and glandular tissue. Sagittal images of female (C) and male (D) tongue worm specimens stained with 0.3% PTA and 1% I_2, respectively. Blue arrow, buccal cavity; green arrows, oesophagus; white arrow, intestine (or midgut). Anterior is to the left (sagittal images) or the top (ventral image). Scanning resolution is 18 μm for all images. White bar = 1 mm. (For interpretation of the references to colour in this figure legend, the reader is referred to the Web version of this article.)

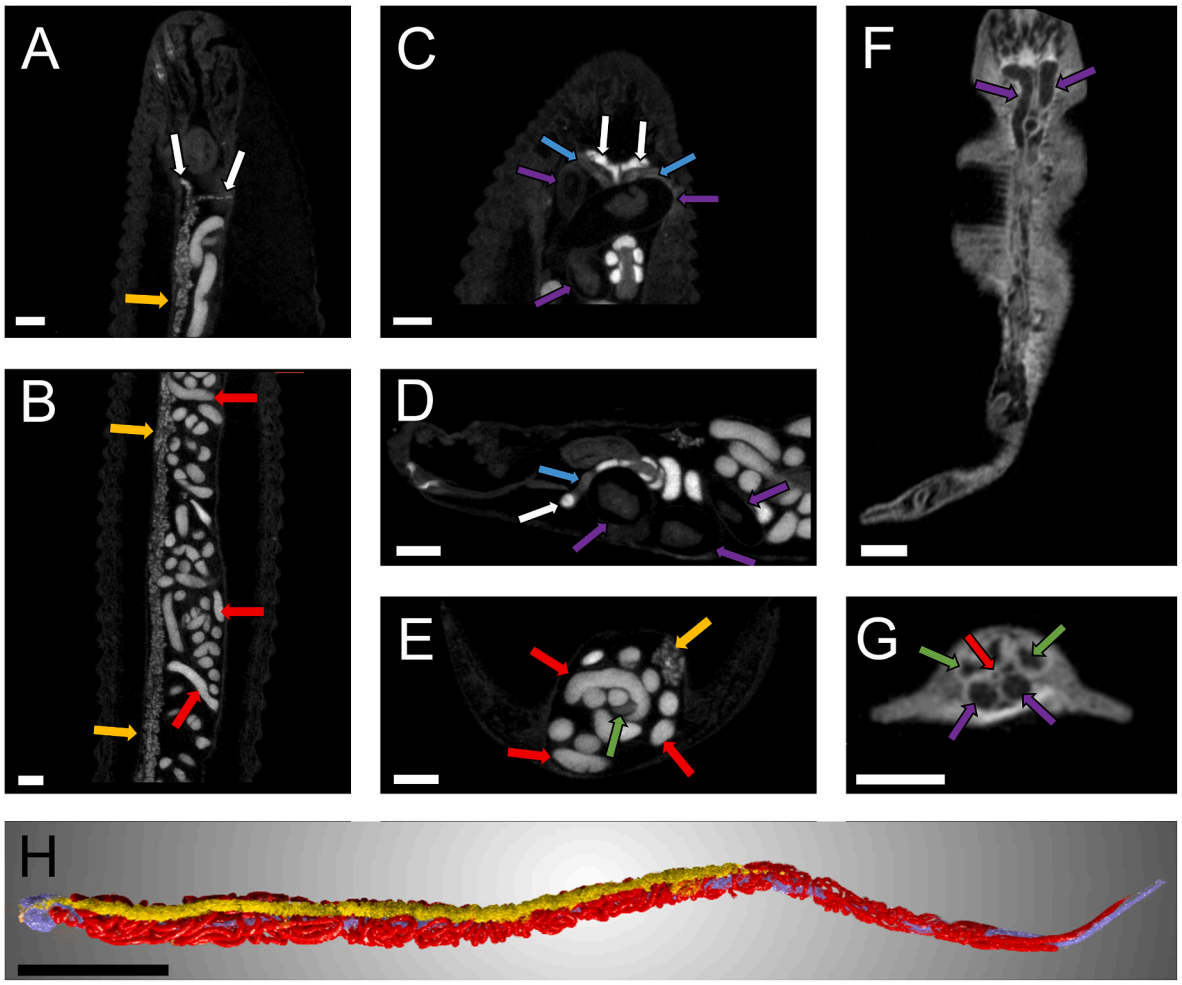

Fig. 9. Dorsal (A & B), ventral (C), sagittal (D) and transversal (E) views of the mid-anterior body of a mature female tongue worm specimen stained with 1% I_2. Ventral (F) and transversal (G) views of a young female specimen stained with 1% I_2. Yellow arrows, ovary; white arrows, oviduct; red arrows, uterus; purple arrows, receptacula seminis; blue arrows, ductules originating from receptacula seminis; green arrow, intestine. (H) 3D volumetric rendering of the ovary (yellow), uterus (red) and intestine (purple) of the mature female tongue worm specimen stained with 1% I_2. In G, note the small size of the uterus (red arrow) in the young female; loops of intestine are seen dorsal to the uterus (green arrows). Anterior is to the top (ventral and dorsal views) or to the left (sagittal views). Scanning resolution for all images is 18 μm. White bar = 1 mm. Black bar = 10 mm. (For interpretation of the references to colour in this figure legend, the reader is referred to the Web version of this article.)

encircled the oesophagus (Fig. 11A–C). Posteriorly, it extended to the distal oviduct/proximal uterus in the female (Fig. 11D) and to the dorsal aspect of the copulatory apparatus in the male (Fig. 11B). The nerves originating from the mass were most clearly seen in a mature female specimen that was stained with 0.3% PTA, and the following description is based on this specimen. There appeared to be nine pairs of nerves, and possibly several smaller nerves, but it was difficult to be certain due to their small size. The nerves were traced as follows, from anterior to posterior: the first pair coursed to the region of the buccal cavity, the second pair to the region of the base of the anterior pair of hooks, the third to the region of the musculature between the hooks, the fourth to the base of the posterior hooks, the fifth to the eighth pair of nerves were small and ran in a transverse direction from the mid-aspect of the sub-oesophageal ganglion and could not be completely followed, and the ninth pair were the largest (known as the abdominal nerve chords) and ran in a posterior direction bilaterally along the ventral coelomic cavity (Fig. 11E).

4. Discussion

This study provided the first anatomical description of *L. serrata* using micro-CT and updated information on *L. serrata* anatomy, particularly its internal anatomy which is only described in a few dated publications. Micro-CT allowed major organ systems to be identified and provided a good gross overview of the coelomic cavity. Micro-CT also enabled visualisation of many of the external characteristics of *L. serrata* previously described by SEM (Shamsi et al., 2020). Sufficient contrast was achieved with both PTA and I_2 stains, and image quality was generally good.

Tongue worms have chitin throughout their bodies including within the external cuticle, hooks, buccal cadre, digestive system, uterus, and copulatory spicules (Spencer, 1892; Mehlhorn, 2008; von Vaupel Klein, 2015; Parija and Chauhury, 2022). Chitin is a strong X-ray absorber and contributes to image contrast. In insects, chitin has been found to impart excellent image contrast, and it is possible to examine insects using micro-CT without additional staining (Killiny and Brodersen, 2022). Staining was found to be necessary with the tongue worms in the current study to achieve sufficient tissue contrast. The hooks, buccal cadre and male copulatory spicules were particularly attenuating, likely reflecting the density of chitin within these structures and the stain uptake.

The stains used, PTA and I_2, are readily available and of low toxicity (Metscher, 2009). The staining protocols were easy to perform and provided adequate tissue contrast. Slight differences were noted between the stains, with 0.1% I_2 providing greater enhancement of the

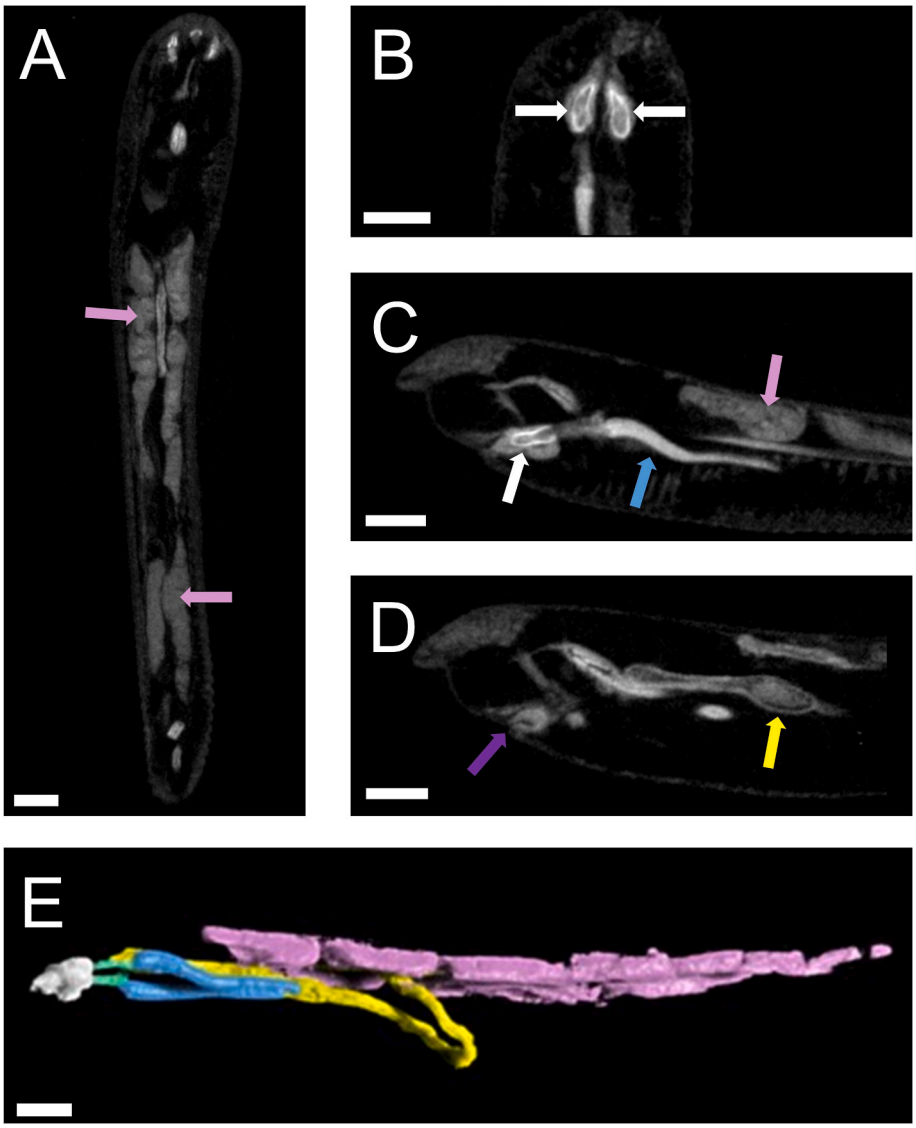

Fig. 10. A male tongue worm specimen stained with 1% I_2; dorsal (A), ventral (B), and sagittal views (C & D). Pink arrows, testes; white arrows, copulatory spicules; blue arrow, ejaculatory duct; yellow arrow, seminal vesicle; purple arrow, genital pore. (E) 3D volumetric rendering of the male reproductive tract: testes (pink), seminal vesicle (yellow), vas deferens (green), ejaculatory ducts (blue), and copulatory spicules (white). Anterior is to the top (dorsal and ventral views) or to the left (sagittal views). Scanning resolution for all images is 18 μm. White bar = 1 mm. (For interpretation of the references to colour in this figure legend, the reader is referred to the Web version of this article.)

hooks, buccal cadre, and copulatory spicules compared to 0.3% PTA. Conversely, in insects, PTA has been found to stain chitin more strongly than I_2 (Metscher, 2009). The differences found in this current study may reflect the staining times used and the diffusion speeds of the stains. I_2 penetrates tissues quickly, while PTA has a moderate diffusion speed (Ondruš et al., 2021). For example, in earthworm specimens, a 3–4 week staining period with 0.3% PTA was required to achieve adequate stain uptake. Specimens stained for shorter durations had prominent internal artifacts (Fernández et al., 2014). In this study, internal structures were adequately stained with 0.3% PTA after 3 days, possibly due to the low density of tongue worms. However, a longer staining time with PTA would likely have resulted in greater stain uptake, particularly of the chitinous structures.

Micro-CT proved to be an efficient and versatile technique. Several specimens were scanned in a relatively short period of time. This allowed anatomical data from various specimens to be compared, and accounted for image datasets that had artifacts and had to be omitted. No overt differences in image quality were observed in specimens that had been fixed in 70% ethanol for up to 4–5 years compared to 12–14 days. Previous studies involving other organisms (e.g., leeches, lampreys) have found that good detail can be achieved even in museum-fixed specimens (Metscher, 2009; Tessler et al., 2016). The main consequence of long-term ethanol fixation is shrinkage and distortion, resulting in measurements not being reliable (Buytaert et al., 2014; Hedrick et al., 2018). Stains can also contribute to specimen shrinkage, particularly high concentrations of iodine (Vickerton et al., 2013; Buytaert et al., 2014).

The main external features of *L. serrata* were visualised with micro-CT, including the hooks, mouth, buccal cadre, hook pits, general body shape, and annuli. They were found to be consistent in appearance with previous descriptions (Shamsi et al., 2020). Pentastome hooks are reported to be hollow; on micro-CT this was appreciated with the hooks having hypoattenuating centres (Bowman, 2013). Finer structures such as papillae, sensillae, and pores that were described on SEM could not clearly be identified with micro-CT (Nikander and Saari, 2006; Shamsi et al., 2020). Image resolution is a limitation with micro-CT (Faulwetter et al., 2013; Fernández et al., 2014). Depending on the system used, it is generally in the range of 0.9–100 μm/pixel, which is coarser than that

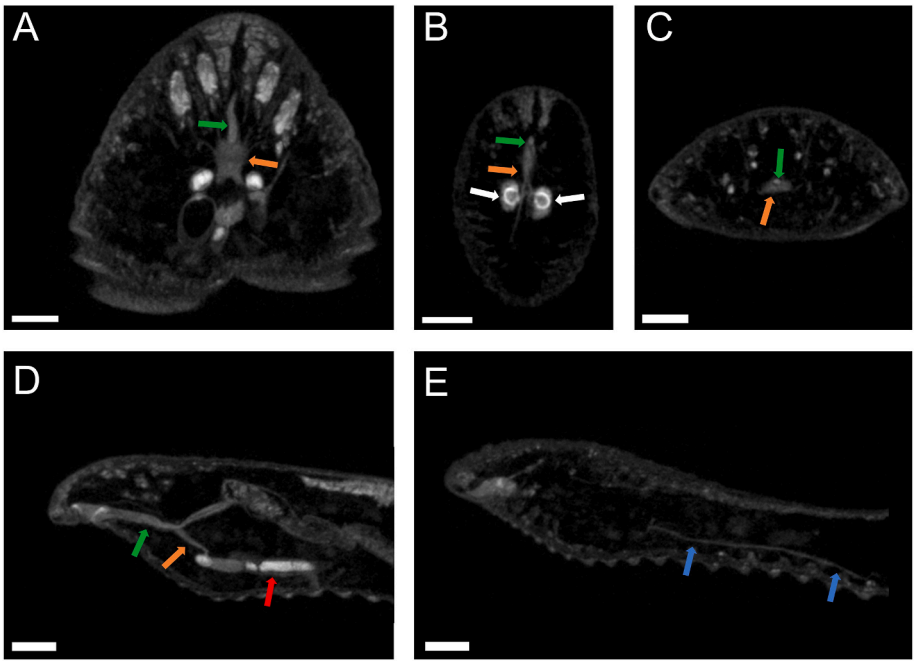

Fig. 11. Ventral (A), transversal (C) and sagittal views (D and E) of the anterior aspect of a female tongue worm specimen stained with 0.3% PTA. (B) A ventral view of the anterior aspect of a male tongue worm specimen stained with 1% I_2. Green arrows, oesophagus; orange arrows, suboesophageal ganglion; white arrows, copulatory spicules; red arrow, uterus; blue arrows, abdominal nerve chord. Anterior is to the top (ventral views) or to the left (sagittal views). Resolution for all images is 18 μm. White bar = 1 mm. (For interpretation of the references to colour in this figure legend, the reader is referred to the Web version of this article.)

provided by SEM and histology (Faulwetter et al., 2013). In this study, 9 μm was the lowest scanning resolution available. Parapar et al. (2017) who assessed the taxonomy of annelids with micro-CT, concluded that micro-CT was most useful for assessing macroscopic external features and gross internal anatomy. When more detailed morphological information is required, complementary imaging techniques such as SEM should be used.

The main organ systems of *L. serrata* (the digestive, reproductive, and nervous) were visualised with micro-CT. The sensory system of pentastomes is reduced, and they do not have respiratory, circulatory, or excretory systems (Nikander and Saari, 2006; von Vaupel Klein, 2015; Parija and Chauhury, 2022). Instead, they have small pores and bacillary cells, which are presumed to be responsible for excretion and respiration (Nikander and Saari, 2006; von Vaupel Klein, 2015). The coelomic space was hypoattenuating, likely reflecting the haemolymph that surrounds the organs. Haemolymph provides a supportive hydrostatic skeleton and facilitates peristaltic locomotion (Paré, 2008; von Vaupel Klein, 2015). The head was dense compared to the rest of the body, with several bands of contrast-enhancing tissue. This is because pentastomids have strong head muscles that, in conjunction with the chitinous plates of the pharynx, allow them to suck and feed from the host (Spencer, 1892; von Vaupel Klein, 2015). Head glands are also reported to intervene between the muscles of the head (Spencer, 1892; von Vaupel Klein, 2015).

Reproductive structures were the dominant internal features of the mature adult tongue worm, particularly the uterus in the female and the testes in the male. The reproductive structures identified with micro-CT, were largely consistent in appearance with previous descriptions of other porocephalid species (Nikander and Saari, 2006; Mehlhorn, 2008; von Vaupel Klein, 2015). Small variations in the female included the receptacula seminis being more elongated and the uterus coiling around the intestine, rather than ventral to the intestine, as depicted by Mehlhorn (2008). Additionally, the ovary was lateralised to one side, rather than running immediately dorsal to the intestine. In the male, the testes were surrounded by a thin tubular structure and the internal testicular tissue was discontinuous. This has been described in *Waddycephalus teretiusculus* (Baird, 1862), another porocephalid species, in which the testis had a thin membranous external layer and scattered multicellular internal masses that were composed of sperm cells at different developmental stages (Spencer, 1892). The seminal vesicle had a slightly tortuous course and was consistent with the description provided by Spencer (1892), who stated it was a tube that "bent double upon itself".

Differences in the reproductive status were noted in the female tongue worms. The uteri contained variable amounts of relatively homogeneous hyperattenuating material. Individual eggs were not visible, likely due to the massive number of eggs present and superimposed upon one another. A gravid porocephalid species is reported to have around 500,000 eggs (Mehlhorn, 2008). In two mature females, the uteri were almost empty, with only a small amount of hyperattenuating material present, possibly reflecting reduced fecundity. Fecundity may be affected by the immunological response of the host and the number of other pentastomids present in an infection (von Vaupel Klein, 2015). One of these females was relatively small (approximately 27 mm in length); age may have been a factor. Alternatively, these females may have recently released a large number of eggs. Sinclair (1954) found that eggs are discharged in host nasal secretions irregularly, but it is not clear how many eggs are released at once.

Micro-CT proved to be a useful technique for determining the sex of the *L. serrata* specimens. One small tongue worm specimen (approximately 15 mm in length) was originally identified as a male when it was retrieved at necropsy due to its small size. Based on the visualisation of its internal organs on micro-CT, it was determined to be a young adult female. The two receptacula seminis were clearly visible and appeared empty. The uterus was small and less coiled compared to that of the mature female, consistent with findings reported by Spencer (1892). There was no evidence of hyperattenuating material (eggs) within the uterus, and the intestine took up relatively more space in the coelomic cavity. The ovary, which has been described as a simple tube in immature females (Spencer, 1892), was not observed in this specimen. Similarly, Fernández et al. (2014) found micro-CT to be useful in determining the sex of juvenile earthworm specimens where external sexual characteristics are often inaccurate.

All components of the digestive tract could be followed with micro-

CT. The pharynx was closely associated with the buccal cadre and not clearly defined, but it appeared to be slightly thicker and more contrast-enhancing than the oesophagus. In pentastomids, the pharynx is described as having a ventral and dorsal chitinous plate, and found to be thicker and stain more readily than the oesophagus (Spencer, 1892; von Vaupel Klein, 2015). The valve between the oesophagus and the intestine, which prevents backflow of ingesta (Mehlhorn, 2008), was clearly visible with micro-CT. The hindgut in pentastome species is described as a short section of intestine, immediately before the anus, that is separated from the midgut by a pyloric valve (Mehlhorn, 2008; von Vaupel Klein, 2015). The hindgut could not be differentiated from the rest of the intestine in this study.

In other porocephalid species, 8–11 pairs of nerves are reported to originate from the suboesophageal ganglion (Doucet, 1965; Mehlhorn, 2008; von Vaupel Klein, 2015). Nine pairs of nerves were identified in this current study; it is likely that some smaller nerves were not visualised because of resolution limitations with micro-CT. Nerves supplying the hooks and the abdominal nerve chords were traced (Doucet, 1965; von Vaupel Klein, 2015).

This study had several limitations. Sample size was small, comprising ten adult *L. serrata* specimens: seven females (one young adult) and three males. There are a limited number of anatomical references on *L. serrata* and porocephalids in general, and anatomical structures were not confirmed through histology. Image quality was generally considered to be good, but was likely affected by a few factors. The specimens had previously been frozen, which is known to alter microstructures (Hu and Xie, 2021). Additionally, the tongue worms were fixed in ethanol, which is known to cause shrinkage of specimens (Vickerton et al., 2013; Buytaert et al., 2014) and soft bodied organisms, such as tongue worm, are particularly prone to distortion during fixation (von Vaupel Klein, 2015). Image contrast may have been improved by using different fixatives; in leeches, glutaraldehyde was found to be superior to ethanol for image resolution (Tessler et al., 2016).

Future micro-CT studies on *L. serrata* could explore other fixatives, stains, and staining times to assess the effect they have on image quality. Using micro-CT to examine different developmental stages, species of *Linguatula*, and tongue worms from other geographical locations, would be beneficial for taxonomic and comparative purposes.

5. Conclusions

This study demonstrated the utility of micro-CT for assessing the anatomy of *L. serrata* and provided updated anatomical information. Good tissue contrast was achieved with both PTA and I_2 stains. Micro-CT was an efficient technique to provide a good gross anatomical overview of the coelomic cavity. Numerous internal and external anatomical structures were visualised and described, including the digestive, reproductive, and nervous systems, as well as the hooks and buccal cadre. Micro-CT could be used in the future to characterise other *Linguatula* species and their developmental stages.

CRediT authorship contribution statement

Alice Birckhead: Writing – review & editing, Writing – original draft, Methodology, Investigation, Formal analysis, Data curation, Conceptualization. **Ryan O'Hare Doig:** Writing – review & editing, Software, Resources, Methodology, Data curation. **Ann Carstens:** Writing – review & editing, Supervision. **David Jenkins:** Writing – review & editing, Supervision, Methodology, Data curation. **Shokoofeh Shamsi:** Writing – review & editing, Supervision.

Funding

This work was supported by the Australian Government Research Training Program Scholarship.

Declaration of competing interest

There is no identifiable Conflict of Interest.

Acknowledgements

The authors acknowledge and thank Dr Diane Barton for helping with some of the initial necropsies and parasite retrievals, and Mrs Cheryl Day from The University of Adelaide for preparing and supplying the phosphotungstic acid and iodine stains used for the micro-CT. Thanks to the vertebrate control officers of the South East NSW Local Lands Services for collecting the fox and wild dog cadavers, from which the tongue worms were retrieved. The authors acknowledge the facilities, and scientific and technical assistance of the National Imaging Facility, a National Collaborative Research Infrastructure Strategy (NCRIS) capability, at the Preclinical, Imaging and Research Laboratories, South Australian Health and Medical Research Institute. We also acknowledge the funding support received from the Australian Government Research Training Program Scholarship.

Appendix 1. Supplementary data

Supplementary data to this article can be found online at https://doi.org/10.1016/j.ijppaw.2024.101002.

References

Attia, M.M., Mahdy, O.A., Soliman, S.M., El-Samannoudy, S.I., Thabit, H., 2024. Morphological and molecular characterization of *Linguatula serrata* and evaluation of the health status of the infested dogs. Comp. Clin. Pathol. 33 (1), 105–114. https://doi.org/10.1007/s00580-023-03527-5.

Barton, D.P., Baker, A., Porter, M., Zhu, X., Jenkins, D., Shamsi, S., 2020. Verification of rabbits as intermediate hosts for *Linguatula serrata* (Pentastomida) in Australia. Parasitol. Res. 119 (5), 1553–1562. https://doi.org/10.1007/s00436-020-06670-y.

Barton, D.P., Gherman, C.M., Zhu, X., Shamsi, S., 2022a. Characterization of tongue worms, *Linguatula* spp.(Pentastomida) in Romania, with the first record of an unknown adult *Linguatula* from roe deer (*Capreolus capreolus Linnaeus*). Parasitol. Res. 121 (8), 2379–2388. https://doi.org/10.1007/s00436-022-07566-9.

Barton, D.P., Porter, M., Baker, A., Zhu, X., Jenkins, D.J., Shamsi, S., 2019. First report of nymphs of the introduced pentastomid, *Linguatula serrata*, in red-necked wallabies (*Notamacropus rufogriseus*) in Australia. Aust. J. Zool. 67 (2), 106–113. https://doi.org/10.1071/ZO20017.

Barton, D.P., Russell, M., Zhu, X., Jenkins, D.J., Shamsi, S., 2021. Verification of the spotted-tail quoll, *Dasyurus maculatus*, as a definitive host for the pentastomid *Linguatula* sp. in Australia. Acta Parasitol. 1–5. https://doi.org/10.1007/s11686-021-00405-4.

Barton, D.P., Shackelford, B., Shamsi, S., Jenkins, D., 2022b. Are feral goats intermediate hosts for *Linguatula* (Pentastomida) in Australia? Int J Parasitol Parasites Wildl 18, 283–286. https://doi.org/10.1016/j.ijppaw.2022.07.004.

Birckhead, A., Jenkins, D., Shamsi, S., Malik, R., Carstens, A., 2024. Intranasal *Linguatula serrata* (tongue worm) in canids and vulpids can be detected using computed tomography. Vet. Radiol. Ultrasound 1–11. https://doi.org/10.1111/vru.13428.

Bowman, D.D. (Ed.), 2013. Georgis' Parasitology for Veterinarians, tenth ed. Elsevier Sauders.

Buytaert, J., Goyens, J., De Greef, D., Aerts, P., Dirckx, J., 2014. Volume shrinkage of bone, brain and muscle tissue in sample preparation for micro-CT and light sheet fluorescence microscopy (LSFM). Microsc. Microanal. 20 (4), 1208–1217. https://doi.org/10.1017/S1431927614001329.

Christoffersen, M.L., De Assis, J.E., 2013. A systematic monograph of the Recent Pentastomida, with a compilation of their hosts. Zool Meded 87 (1), 1–206.

Doucet, J., 1965. Contribution à l'étude anatomique, histologique et histochimique des pentastomes (Pentastomida). ORSTOM.

Faulwetter, S., Vasileiadou, A., Kouratoras, M., Dailianis, T., Arvanitidis, C., 2013. Micro-computed tomography: introducing new dimensions to taxonomy. ZooKeys 263, 1–45. https://doi.org/10.3897/zookeys.263.4261.

Fernández, R., Kvist, S., Lenihan, J., Giribet, G., Ziegler, A., 2014. Sine systemate chaos? A versatile tool for earthworm taxonomy: non-destructive imaging of freshly fixed and museum specimens using micro-computed tomography. PLoS One 9 (5), e96617. https://doi.org/10.1371/journal.pone.0096617.

Giglio, A., Vommaro, M.L., Agostino, R.G., Lo, L.K., Donato, S., 2022. Exploring compound eyes in adults of four coleopteran species using synchrotron X-ray phase-contrast microtomography (SR-PhC micro-CT). Life 12 (5), 741. https://doi.org/10.3390/life12050741.

Gignac, P.M., Kley, N.J., Clarke, J.A., Colbert, M.W., Morhardt, A.C., Cerio, D., Cost, I.N., Cox, P.G., Daza, J.D., Early, C.M., 2016. Diffusible iodine-based contrast-enhanced computed tomography (diceCT): an emerging tool for rapid, high-resolution, 3-D imaging of metazoan soft tissues. J. Anat. 228 (6), 889–909.

Haffner, K.V., Rack, G., Sachs, R., 1969. Verschiedene vertreter der Familie Linguatulidae (pentastomida) als parasiten von Säugetieren der Serengeti (anatomie, systematik, biologie). Mitt Staatsinst Zool Mus Hambg 66, 93–144.

Hedrick, B.P., Yohe, L., Vander Linden, A., Dávalos, L.M., Sears, K., Sadier, A., Rossiter, S.J., Davies, K.T.J., Dumont, E., 2018. Assessing soft-tissue shrinkage estimates in museum specimens imaged with diffusible iodine-based contrast-enhanced computed tomography (diceCT). Microsc. Microanal. 24 (3), 284–291. https://doi.org/10.1017/S1431927618000399.

Hu, C., Xie, J., 2021. The effect of multiple freeze-thaw cycles on the microstructure and quality of *Trachurus murphyi*. Foods 10 (6), 1350. https://doi.org/10.3390/foods10061350.

Killiny, N., Brodersen, C.R., 2022. Using x-ray micro-computed tomography to three-dimensionally visualize the foregut of the Glassy-Winged Sharpshooter (*Homalodisca vitripennis*). Insects 13 (8), 710. https://doi.org/10.3390/insects13080710.

Lee, C.H., Im, J.-G., Goo, J.M., Lee, H.J., Hong, S.-T., Shen, C.H., Chung, D.H., Son, K.R., Chang, J.M., Eo, H., 2007. Serial CT findings of *Paragonimus* infested dogs and the Micro-CT findings of the worm cysts. Korean J. Radiol. 8 (5), 372–381. https://doi.org/10.3348/kjr.2007.8.5.372.

Mehlhorn, H. (Ed.), 2008. Encyclopedia of Parasitology, 3 ed. Springer, Berlin.

Metscher, B.D., 2009. MicroCT for comparative morphology: simple staining methods allow high-contrast 3D imaging of diverse non-mineralized animal tissues. BMC Physiol. 9 (11). https://doi.org/10.1186/1472-6793-9-11.

Nikander, S., Saari, S., 2006. A SEM study of the reindeer sinus worm (*Linguatula arctica*). Rangifer 26 (1), 15–24. https://doi.org/10.7557/2.26.1.197.

Noever, C., Keiler, J., Glenner, H., 2016. First 3D reconstruction of the rhizocephalan root system using MicroCT. J. Sea Res. 113, 58–64. https://doi.org/10.1016/J.SEARES.2015.08.002.

O'Sullivan, J., Cruickshank, S., Withers, P., Else, K., 2021. Morphological variability in the mucosal attachment site of *Trichuris muris* revealed by X-ray microcomputed tomography. Int. J. Parasitol. 51 (10), 797–807. https://doi.org/10.1016/j.ijpara.2021.04.006.

O'Sullivan, J.D.B., Behnsen, J., Starborg, T., MacDonald, A.S., Phythian-Adams, A.T., Else, K.J., Cruickshank, S.M., Withers, P.J., 2018. X-ray micro-computed tomography (μCT): an emerging opportunity in parasite imaging. Parasitology 145 (7), 848–854. https://doi.org/10.1017/S0031182017002074.

Ondruš, J., Hubatka, F., Kulich, P., Odehnalová, N., Harabiš, V., Hesko, B., Sychra, O., Široký, P., Turánek, J., Novobilský, A., 2021. A novel approach to imaging engorged ticks: micro-CT scanning of *Ixodes ricinus* fed on blood enriched with gold nanoparticles. Ticks Tick Borne Dis 12 (1), 101559. https://doi.org/10.1016/j.ttbdis.2020.101559.

Parapar, J., Candás, M., Cunha-Veira, X., Moreira, J., 2017. Exploring annelid anatomy using micro-computed tomography: a taxonomic approach. Zool. Anz. 270 (82), 19–42. https://doi.org/10.1016/j.jcz.2017.09.001.

Paré, J.A., 2008. An overview of pentastomiasis in reptiles and other vertebrates. J. Exot. Pet Med. 17 (4), 285–294. https://doi.org/10.1053/J.JEPM.2008.07.005.

Parija, S.C., Chauhury, A. (Eds.), 2022. Textbook of Parasitic Zoonoses, 1 ed. Springer, Singapore. https://doi.org/10.1007/978-981-16-7204-0.

Rezaei, F., Tavassoli, M., Hashemnia, M., Naem, S., Gholizadeh, M., 2016. Some morphological data of various stages of *Linguatula serrata*. İstanbul Üniversitesi. Veteriner Fakültesi Dergisi 42 (1), 38–46. https://doi.org/10.16988/iuvfd.2016.48454.

Rother, L., Kraft, N., Smith, D.B., El Jundi, B., Gill, R.J., Pfeiffer, K., 2021. A micro-CT-based standard brain atlas of the bumblebee. Cell Tissue Res. 386, 29–45. https://doi.org/10.1007/s00441-021-03482-z.

Sambon, L.W., 1922. A synopsis of the family Linguatulidae. J. Trop. Med. Hyg. 25 (24).

Shamsi, S., Barton, D.P., Zhu, X., Jenkins, D.J., 2020. Characterisation of the tongue worm, *Linguatula serrata* (pentastomida: linguatulidae), in Australia. Int J Parasitol Parasites Wildl 11, 149–157. https://doi.org/10.1016/j.ijppaw.2020.01.010.

Shamsi, S., McSpadden, K., Baker, S., Jenkins, D.J., 2017. Occurrence of tongue worm, *Linguatula cf. serrata* (Pentastomida: linguatulidae) in wild canids and livestock in south-eastern Australia. Int J Parasitol Parasites Wildl 6 (3), 271–277. https://doi.org/10.1016/j.ijppaw.2017.08.008.

Shamsi, S., Zhu, X., Halajian, A., Barton, D.P., 2022. 28S rRNA sequences for *Linguatula* spp. Parasitol. Res. 121 (6), 1799–1804. https://doi.org/10.1007/s00436-022-07507-6.

Sinclair, K.B., 1954. The incidence and life cycle of *Linguatula serrata* (Frohlich 1789) in Great Britain. J. Comp. Pathol. 64 (4), 371–383. https://doi.org/10.1016/s0368-1742(54)80038-5.

Smith, D.B., Bernhardt, G., Raine, N.E., Abel, R.L., Sykes, D., Ahmed, F., Pedroso, I., Gill, R.J., 2016. Exploring miniature insect brains using micro-CT scanning techniques. Sci. Rep. 6 (1), 21768. https://doi.org/10.1038/srep21768.

Spencer, W.B., 1892. Memoirs: the anatomy of pentastomum teretiusculum (Baird). J. Cell Sci. 2 (133), 1–74.

Tabaripour, R., Keighobadi, M., Sharifpour, A., Azadeh, H., Shokri, A., Banimostafavi, E. S., Fakhar, M., Abedi, S., 2021. Global status of neglected human *Linguatula* infection: a systematic review of published case reports. Parasitol. Res. 120 (9), 3045–3050. https://doi.org/10.1007/s00436-021-07272-y.

Tabaripour, R., Shokri, A., Teshnizi, S.H., Fakhar, M., Keighobadi, M., 2019. Status of *Linguatula serrata* infection in livestock: a systematic review with meta-analysis in Iran. Parasite Epidemiol Control 7, e00111. https://doi.org/10.1016/j.parepi.2019.e00111.

Tessler, M., Barrio, A., Borda, E., Rood-Goldman, R., Hill, M., Siddall, M.E., 2016. Description of a soft-bodied invertebrate with microcomputed tomography and revision of the genus Chtonobdella (Hirudinea: haemadipsidae). Zool Scr 45 (5), 552–565. https://doi.org/10.1111/zsc.12165.

Vickerton, P., Jarvis, J., Jeffery, N., 2013. Concentration-dependent specimen shrinkage in iodine-enhanced micro CT. J. Anat. 223 (2), 185–193. https://doi.org/10.1111/joa.12068.

von Vaupel Klein, C. (Ed.), 2015. Treatise on Zoology- Anatomy, Taxonomy, Biology. The Crustacea, vol. 5. Brill.